OPTIMIZATION OF FUZZY PID CONTROL USING AN IMPROVED SPARROW SEARCH ALGORITHM FOR SOYBEAN FOLIAR FERTILIZER SPRAYING
/
基于改进麻雀搜索算法的大豆叶面肥喷施模糊 PID 控制优化研究

Yue CHEN[1)], Hailiang GONG[1)], Weidong ZHUANG*[1)]
College of Engineering, Heilongjiang Bayi Agricultural University, Daqing, Heilongjiang, 163319, China
Tel: 13836962853; E-mail: 81nd@163.com
DOI: https://doi.org/10.35633/inmateh-79-50

***Keywords**: Variable-rate application; Hydraulic actuator; Sparrow search algorithm; Dynamic response; Precision agriculture*

ABSTRACT
To address the low control precision caused by the high nonlinearity and pure time-delay of hydraulic pipelines in variable-rate soybean foliar fertilization, this study developed an automatic variable-rate control system for boom sprayers. Based on Fluent dynamic mesh simulations, the throttling characteristics of the electric control valve were revealed, and a second-order transfer function model with pure time-delay was accurately identified for the actuator. To overcome the reliance of conventional fuzzy controllers on expert experience, an improved Sparrow Search Algorithm-optimized Fuzzy PID (ISSA-Fuzzy PID) control strategy was proposed. By integrating optimized population initialization and adaptive global search, this improvement mechanism effectively avoids premature convergence during dynamic parameter tuning. Simulation results indicate that the proposed algorithm compresses the rise time to 0.35 s, limits the overshoot to within 20%, and achieves steady-state convergence within 1.0 s. Bench tests verified that the average detection errors for system flow rate and pressure were merely 2.14% and 2.34%, respectively. Under the working pressure of 250–350 kPa, dynamic pressure regulations were completed stably within 1.9 s without significant overshoot, exhibiting improved regulation precision under high-flow conditions. This research effectively overcomes the lag bottleneck of actuating mechanisms, providing an integrated control solution with high dynamic response and steady-state precision for variable-rate applications. Practically, this optimized system ensures rapid dosage correction and pressure stability, providing technical support for improving the operational timeliness and fertilizer-use efficiency of field spraying operations.

摘 要
针对大豆叶面肥变量喷施中液压管路高非线性与纯滞后导致的控制精度低等问题，本文开发了一套喷杆喷雾机变量自动控制系统。基于 Fluent 动网格仿真揭示了电控阀节流特性，并精确辨识出执行机构的二阶带纯滞后传递函数模型。为克服模糊控制器高度依赖专家经验的局限，提出改进麻雀搜索算法优化模糊 PID（ISSA-Fuzzy PID）控制策略。该改进机制通过融合优化的种群初始化与自适应全局搜索策略，有效避免了动态参数寻优过程中的早熟收敛问题。仿真表明，该算法将上升时间缩短至 0.35 s，超调量控制在 20% 以内，并在 1.0 s 内实现稳态收敛。台架试验验证：系统流量与压力的平均误差仅为 2.14% 和 2.34%；在 250~350 kPa 工作压力下，动态调节可在 1.9 s 内无显著超调地切入稳态，且大流量工况下调节精度更优。本研究有效突破了执行机构的滞后瓶颈，为高精度变量施药提供了兼具高动态响应与稳态精度的集成控制方案。在实际应用中，该系统能够确保施药量的快速修正与压力稳定，从而显著提升田间喷施作业的响应及时性与肥料利用率。

INTRODUCTION
The integration of base fertilizer application and precision foliar spraying represents a transformative shift in modern agricultural development (*Farooque et al., 2023*). Foliar fertilization enhances nutrient utilization efficiency, directly influencing crop physiological development, yield, and grain quality. Despite these benefits, traditional uniform spraying methods fail to account for spatial heterogeneities in soil fertility and crop nutrient requirements. Consequently, excessive application leads to environmental degradation, whereas under-application limits yield potential. To mitigate these issues, transitioning from uniform application to high-precision, variable-rate application (VRA) is imperative for sustainable agricultural production (*Yuxuan et al., 2025*).

Historically, VRA systems have relied heavily on pre-generated prescription maps. Although these maps support the optimization of spatial input distribution, their generation is labor-intensive, and their static nature prevents adaptation to dynamic field conditions in real time *(Pawase et al., 2023; Dong et al., 2025)*. This limitation has catalyzed a research trend toward real-time sensor-based feedback loops and advanced control algorithms. Extensive reviews on intelligent variable-rate spray technologies confirm that multi-variable coupling decision-making models and real-time execution remain the core direction of global agricultural engineering (*Jiao et al., 2025*). Among existing controllers, PID remains a standard, yet its performance is frequently compromised by system nonlinearities and time lags inherent in hydraulic sprayers. To overcome these deficiencies, recent studies have successfully utilized single-neuron architectures (*Su et al., 2022*) and intelligent optimization methods, such as incremental PID for side-deep fertilization (*Xie et al., 2026*) and PSO-based Fuzzy-PID for real-time regulation (*Xu et al., 2025*).

However, a critical comparison of recent AI-based control strategies reveals significant trade-offs regarding their suitability for low-cost agricultural machinery. Advanced machine learning policies typically necessitate extensive interaction data and high computational power, posing implementation challenges for embedded spraying terminals (*Dhanya et al., 2022*). Similarly, while neural-network PID tuning improves nonlinear approximation, these models often lack interpretability, complicating maintenance when hydraulic components degrade *(Zhu et al., 2023*). In contrast, Swarm-Intelligence-optimized Fuzzy PID control offers a pragmatic compromise: it maintains rule-based interpretability and low computational cost while leveraging global search capabilities for parameter optimization. This approach is heavily validated in the latest precision agricultural research. For example, recent works have demonstrated superior self-correcting fuzzy PID control for integrated water-fertilizer irrigation (*Zhang et al., 2025*), and Tuna Swarm Optimization (TSO) combined with Fuzzy PID has been reported to improve remote fertilization flow control and reduce overshoot (*Wu et al., 2026*).

Despite these advancements, rapid, stable, and precise real-time control tailored for soybean foliar fertilization remains elusive. Existing systems are frequently hindered by a combination of technical bottlenecks: prescription-map latency, nonlinear valve throttling, pure time-delay in long hydraulic pipelines, pressure pulsation from diaphragm pumps, and insufficient controller robustness under fluctuating flow demands. Therefore, this study tests the hypothesis that an improved Sparrow Search Algorithm (SSA) *(Xu et al., 2025*) optimized Fuzzy PID controller can significantly reduce transient response times and suppress overshoot compared to conventional PID and manually tuned controllers. To validate this, we propose an automatic boom sprayer control system integrating an improved SSA with a fuzzy PID strategy. To validate this approach, an automatic boom-sprayer control system integrating an improved SSA with a fuzzy PID control strategy is developed. By utilizing a GreenSeeker spectral sensor for real-time monitoring of crop growth status (*Patle et al., 2025*), the system facilitates immediate variable-rate topdressing, bypassing map latency and enhancing the precision of foliar fertilization practices.

MATERIALS AND METHODS

Structure and Principle of the Automatic Spraying Control System

The automatic spraying control system utilizes a spectral sensor at the front end to collect soybean NDVI data, which are transmitted via the CAN bus to an upper computer for analysis, thereby assisting the intelligent control terminal in making spraying decisions. At the rear end, an electronically controlled regulating valve is employed as the control component to achieve the regulation of pipeline pressure and flow rate. Upon receiving commands from the onboard intelligent control terminal, the motion controller outputs an analog voltage signal to regulate the electronically controlled valve. This adjusts the valve spool position, thereby modulating the opening degree of the valve. Changes in flow rate and pressure within the system pipeline are monitored by a flow sensor and a pressure transmitter, respectively, with the recorded data transmitted to the control terminal. The electronically controlled regulating valve continuously modulates the flow rate and pressure within the pipeline. Meanwhile, the motion controller collects signals from the sensors and receives commands from the upper computer to control the valve's on/off state and opening degree. The system structure schematic is shown in Fig. 1.

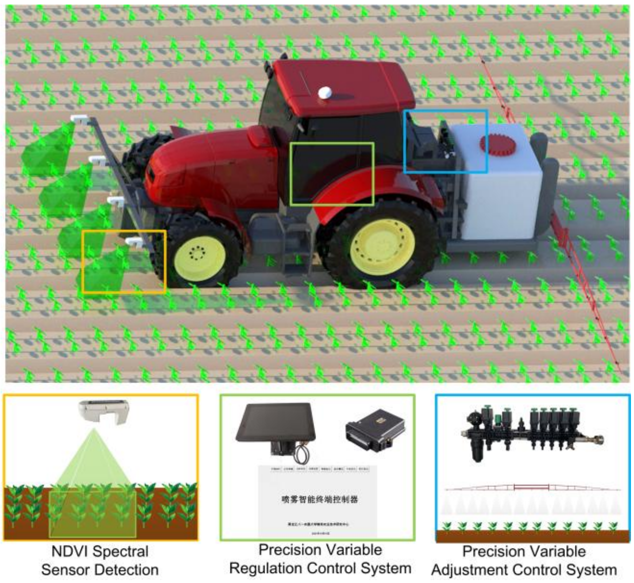

Fig. 1 - Schematic diagram of the system structure

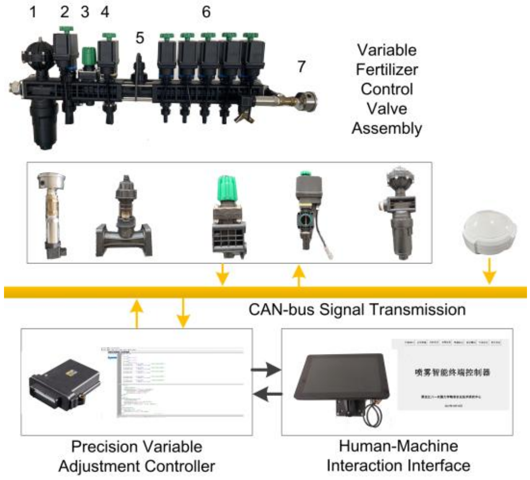

1.Pressure Regulator Filter; 2. Electric Main Valve; 3. Manual Pressure Regulating Valve; 4. Electronic Control Valve; 5. Flow Sensor; 6. Electronic Control Branch Valve; 7. Pressure Sensor

Fig. 2 - Control valve assembly of the spraying system

Test Equipment

The control valve assembly of the automatic system utilized a product manufactured by Ningbo Licheng Agricultural Spraying Technology Co., Ltd., China (Fig. 2). This assembly ensures stable sprayer operation by integrating pressure stabilization, filtration, regulation, and pipeline flow distribution. In this system, the motion controller adjusts the spool opening of the electric control valve based on target commands. This alters the pressure within the flow channel, modulating the flow velocity to achieve precise variable-rate spraying.

Simulation of automatic spraying control system

To investigate the flow velocity and pressure fields within the flow channel and analyze the energy loss caused by the valve's intrinsic structural characteristics, ANSYS Fluent computational fluid dynamics (CFD) simulation was employed. This analysis provides a theoretical foundation for subsequent system adjustments and algorithm calibration.

3D modeling and mesh generation

Based on the structural parameters of the electronically controlled regulating valve, a 3D model was constructed in UG (Fig. 3), and its fluid domain was extracted and meshed for fluid dynamics analysis (Fig. 4). During operation, the foliar fertilizer enters through the valve inlet, is modulated by the valve spool, and exits via the outlet. A motor drives the spool vertically to a predetermined opening angle, altering the annular gap between the guiding spool and the valve body.

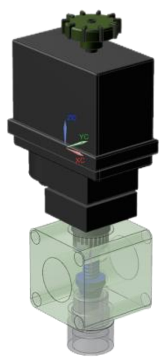

Fig. 3 - Three-dimensional model of the electronic control valve

Fig. 4 - Fluid domain mesh division

Given that the foliar fertilizer liquid is incompressible, a pressure-based solver was adopted. The inlet of the valve was defined as a pressure inlet, the outlet as a pressure outlet, and a no-slip condition was applied to all internal pipe walls.

For reproducibility, the CFD workflow was supplemented as follows. The valve fluid domain was discretized with an unstructured tetrahedral mesh and local refinement near the valve-core throttling region and wall boundary layers. Three mesh densities were compared during mesh-independence checking, and the final grid was selected when the outlet-flow variation between two adjacent refinements was below 2 %. The final model contained approximately 3.2 × 10^5 cells, the minimum orthogonal quality was greater than 0.20, and the maximum skewness was less than 0.85. The SIMPLE pressure-velocity coupling scheme and second-order upwind discretization were used, and each operating condition was iterated until scaled residuals for continuity and momentum were below 1.0 × 10^{-5} and the outlet-flow monitor became stable.

Turbulence modeling and dynamic mesh

The flow regime of the liquid is determined by the Reynolds number (Re), defined as:

$$Re = \frac{\rho v D}{\mu} \tag{1}$$

where ρ represents the fluid density, v is the fluid velocity, D is the pipe diameter, and μ is the fluid dynamic viscosity.

Calculations yielded an Re of 9726. Because $Re \geq 8000$, the fluid flow transitions to a fully turbulent state, necessitating the standard k-ε turbulence model for calculations. The standard k-ε model is a fully turbulent computational model that disregards the influence of molecular viscosity. By coupling turbulent kinetic energy and dissipation rate, it determines the distribution of velocity, pressure, and energy, enabling precise simulation of turbulent flow at intermediate-to-high Reynolds numbers. Furthermore, to simulate the continuous adjustment of the electric control valve, a dynamic grid method utilizing a dynamic layering approach (cell size of 0.002 m) was employed at the rigid interface, while all other variables were set to their default values.

Design of the ISSA-Fuzzy PID Control Algorithm

In the operational process of the variable-rate spray system, inherent pure time-delay and nonlinear characteristics emerge due to the response latency of the electric control valve, pressure regulation dynamics, and flow stabilization time. Conventional proportional-integral-derivative (PID) controllers struggle to handle such time-delay systems effectively, often resulting in severe overshoot and poor robustness (*Karimi et al., 2004*). To eliminate the hysteresis effect and enhance the dynamic precision of the spraying control system, this study proposes an advanced Sparrow Search Algorithm optimized Fuzzy PID (ISSA-Fuzzy PID) control strategy.

System Identification of the Actuator

Establishing an accurate mathematical model is a prerequisite for robust control system design. In this study, system identification was employed to derive the equivalent transfer function of the electric control valve. Fluent computational fluid dynamics (CFD) simulations, combined with dynamic mesh techniques, were conducted on the core components of the variable-rate system (*Kumar et al., 2021*). Analyzing the simulated transient response data revealed that the actuator exhibits second-order dynamic characteristics.

Consequently, a second-order transfer function structure was selected for the spraying automatic control system. The System Identification Toolbox in MATLAB 2020 was utilized for offline parameter identification. The input-output data pairs from the Fluent simulations were imported into the MATLAB workspace, with the transfer function order set to 2 and the number of zeros set to 0. Based on the CFD simulation data, the identified continuous-time transfer function is expressed as Eq. (2):

$$G_{sim}(s) = \frac{K_{sim}}{T_1 s^2 + T_2 s + 1} e^{-\tau_{sim} s} \tag{2}$$

where $G_{sim}(s)$ represents the simulated transfer function of the actuator; K_{sim} is the system gain derived from the simulation; T_1 and T_2 denote the time constants of the second-order system; τ_{sim} represents the pure time delay reflecting the response latency; and s is the Laplace complex variable.

Model validation through MATLAB demonstrated a fitting accuracy of 89.91%, verifying the reliability of the identification. Furthermore, utilizing the actual input-output data acquired from the physical performance tests, an empirical system identification was conducted to derive the practical transfer function, as shown in Eq. (3):

$$G_{\exp}(s) = \frac{K_{\exp}}{T_3 s^2 + T_4 s + 1} e^{-\tau_{\exp} s} \tag{3}$$

where $G_{\exp}(s)$ is the empirical transfer function obtained from physical experiments; $K_{\exp}$ represents the actual system gain; T_3 and T_4 are the experimental time constants; and $\tau_{\exp}$ is the actual pure time delay of the hardware system.

Conventional PID Control Model

The PID controller regulates the system output by calculating the proportion (P), integral (I), and derivative (D) of the error between the measured output and the desired target value (*Zhu et al., 2023*). The schematic diagram of the control system is shown in Fig. 5.

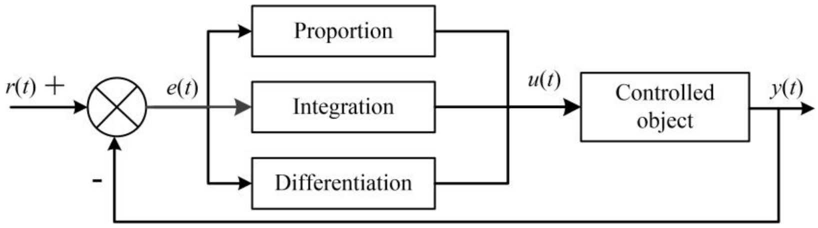

Fig. 5 - Schematic diagram of the PID control system

The error signal $e(t)$ between the system reference input $r(t)$ and the actual output $y(t)$ is defined in Eq. (4):

$$e(t) = r(t) - y(t) \tag{4}$$

The standard position PID control law, which continuously minimizes the error $e(t)$ to achieve the system's control objective, is expressed in Eq. (5):

$$u(t) = K_p\left[e(t) + \frac{1}{T_i}\int_0^t e\,(\tau)d\tau + T_d\frac{de(t)}{dt}\right] \tag{5}$$

where $u(t)$ represents the control output signal; K_p is the proportional gain; T_i denotes the integral time constant; and T_d represents the derivative time constant.

Sparrow Search Algorithm Optimized Fuzzy PID Control

The Sparrow Search Algorithm (SSA) is a swarm intelligence optimization technique inspired by the foraging and anti-predation behaviors of sparrows (*Xue and Shen, 2020*). By simulating these behaviors, the algorithm treats the solution space of the optimization problem as a foraging area, skillfully balancing global exploration with local exploitation. The population is divided into three functional roles: producers, scroungers, and scouts. Producers are responsible for locating optimal food sources and guiding the population. Scroungers follow the producers to exploit resources while monitoring environmental changes. Simultaneously, scouts act as an early-warning mechanism; upon detecting a predator, they issue alarm signals, prompting the population to evacuate. This division of labor endows the SSA with rapid convergence, strong adaptability, and exceptional global search capabilities.

The primary mission of the producers is to provide orientation and indicate food sources for the entire population. The position update rule for producers is given by Eq. (6):

$$X_{i,j}^{t+1} = \begin{cases} X_{i,j}^t \exp\left(-\frac{i}{\alpha iter_{\max}}\right), R_2 < ST \\ X_{i,j}^t + Q \cdot L, \qquad R_2 \geq ST \end{cases} \tag{6}$$

where $X_{i,j}$ denotes the position of the i-th sparrow in the j-th dimension; t represents the current iteration; $iter_{\max}$ is the maximum number of iterations; α is a uniformly distributed random number in $(0,1]$; $R_2 \in [0,1]$ represents the alarm value; $ST \in [0.5,1]$ is the safety threshold; Q is a random number generated from a normal distribution; and L is a $1 \times d$ matrix with all elements equal to 1. When $R_2 < ST$, the environment is safe, and producers conduct an extensive search; when $R_2 \geq ST$, danger is detected, and the population immediately relocates to a safe area.

The position update for the scroungers is defined by Eq. (7):

$$X_{i,j}^{t+1} = \begin{cases} Q \cdot \exp\left(\frac{X_{worst}^t - X_{i,j}^t}{i^2}\right), & i > \frac{n}{2} \\ X_{best}^{t+1} + \left|X_{i,j}^{t+1} - X_{best}^{t+1}\right| \cdot A^+ \cdot L, & i \leq \frac{n}{2} \end{cases} \tag{7}$$

where X_{worst} denotes the global worst position in the current iteration; X_{best} represents the optimal position occupied by the producers; A is a multi-dimensional row matrix with elements randomly assigned 1 or -1, satisfying $A^+ = A^T(AA^T)^{-1}$; and n denotes the population size. When $i > n/2$, it indicates that the scrounger is in a poor location and must forage elsewhere.

The position update for the scouts is given by Eq. (8):

$$X_{ij}^{t+1} = \begin{cases} X_{best}^{t} + \beta \cdot \left| X_{ij}^{t} - X_{best}^{t} \right|, & f_i > f_g \\ X_{ij}^{t} + K \cdot \left(\frac{\left| X_{ij}^{t} - X_{worst}^{t} \right|}{f_i - f_w + \varepsilon} \right), & f_i = f_g \end{cases} \tag{8}$$

where β is a step control parameter following a standard normal distribution; X_{best} denotes the current global optimal position; $K \in [-1,1]$ is a random step parameter specifying the direction of movement; f_i is the fitness value of the i-th sparrow; and f_g and f_w are the current global best and worst fitness values, respectively. ε is a negligible constant to prevent division by zero.

In conventional fuzzy PID control, the formulation of fuzzy rules and scaling factors relies heavily on expert experience, which introduces subjectivity and limits real-time adaptability (*Xu et al., 2025*). This often leads to sub-optimal tuning of PID parameters, slowing down the system response and making it inadequate for the highly dynamic variable-rate spraying system. To overcome this, the SSA is employed to dynamically optimize the quantization factors (K_{E}, K_{EC}) and the PID parameters (K_p, K_i, K_d) within the fuzzy controller. The principle of the ISSA-Fuzzy PID controller is illustrated in Fig. 6.

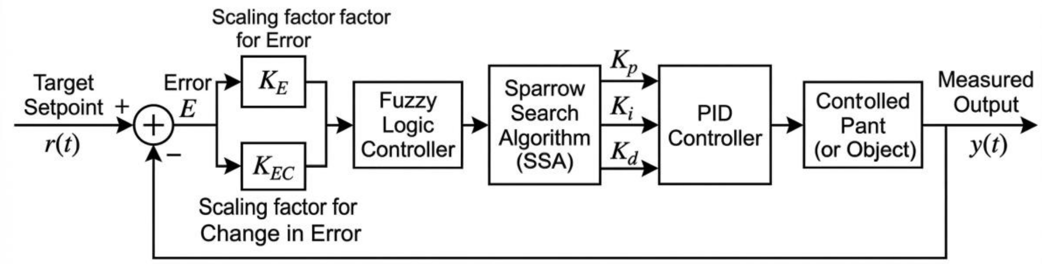

Fig. 6 - Schematic diagram of the Sparrow Search optimized fuzzy PID controller

To evaluate the optimization process, an integral objective function is defined. To prevent excessive control amplitudes and actuator saturation, the objective function integrates the absolute error and the control signal $u(t)$, as shown in Eq. (9):

$$J_1 = \int_0^{\infty} \left(w_1 \cdot t|e(t)| + w_2 \cdot u^2(t) + w_3 \cdot |e(t)| \right) dt \tag{9}$$

where w_1, w_2, w_3 denote the assigned parameter weight values used to balance the tracking performance and energy consumption.

Fuzzy Logic Design and SSA Optimization Parameters

The fuzzy controller utilizes the system error e and the error change rate ec as input variables. The input signals undergo a fuzzification process, followed by fuzzy inference based on established control rules. Finally, the centroid method is employed for defuzzification to output the precise PID parameter compensation increments: $\Delta\mathrm{K_p}, \Delta\mathrm{K_i}, \text{and } \Delta\mathrm{K_d}$.

The fuzzy input universe of discourse for both the system error and the error change rate is defined as [-2, 2], while the fuzzy output universe for K_p, K_i, and K_d is constrained to [-1, 1]. Both input and output variables are partitioned into seven fuzzy subsets (linguistic variables): Negative Big (NB), Negative Medium (NM), Negative Small (NS), Zero (ZO), Positive Small (PS), Positive Medium (PM), and Positive Big (PB). To ensure the sensitivity and computational efficiency of the control system, triangular membership functions with high distinguishability are universally adopted across the entire universe of discourse. Fig. 7 and Fig. 8 illustrate the membership functions for the input and output variables, respectively.

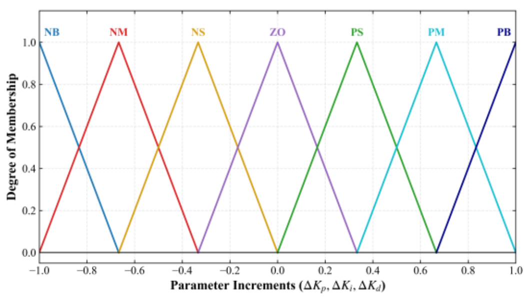

Fig. 7 - Membership functions of input variables

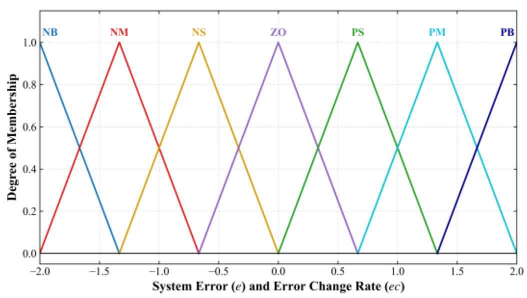

Fig. 8 - Membership functions of output variables

Fuzzy control rules form the core of the fuzzy inference mechanism, directly determining the dynamic performance of the control system. Rational rule configuration effectively enhances system stability, minimizes overshoot, and reduces the settling time. Tailored to the direct current (DC) motor-driven actuator, 49 IF-THEN fuzzy control rules were extracted based on expert experience, as detailed in Table 1.

Table 1

Fuzzy rule base for PID parameter increments

E \ EC	NB	NM	NS	ZO	PS	PM	PB
NB	PB/NB/PS	PB/NB/NS	PM/NM/NB	PM/NM/NB	PS/NS/NB	ZO/ZO/NM	ZO/ZO/PS
NM	PB/NB/PS	PB/NB/NS	PM/NM/NB	PS/NS/NM	PS/NS/NM	ZO/ZO/NS	NS/ZO/ZO
NS	PM/NB/ZO	PM/NM/NS	PM/NS/NM	PS/NS/NM	ZO/ZO/NS	NS/PS/NS	NS/PS/ZO
ZO	PM/NM/ZO	PM/NM/NS	PS/NS/NS	ZO/ZO/NS	NS/PS/NS	NM/PM/NS	NM/PM/ZO
PS	PS/NM/ZO	PS/NS/ZO	ZO/ZO/ZO	NS/PS/ZO	NS/PS/ZO	NM/PM/ZO	NM/PB/ZO
PM	PS/ZO/PB	ZO/ZO/NS	NS/PS/PS	NM/PM/PS	NM/PM/PS	NM/PB/PS	NB/PB/PB
PB	ZO/ZO/PB	ZO/ZO/PM	NM/PS/PM	NM/PM/PM	NM/PB/PS	NB/PB/PS	NB/PB/PB

To achieve global parameter optimization, the Sparrow Search Algorithm (SSA) is employed to optimize the scaling factors and the baseline PID parameters of the fuzzy controller. The specific hyperparameters of the algorithm are configured as follows: the population size is set to 30, and the maximum number of iterations is 100. The proportions of producers, scroungers, and scouts within the population are set to 20%, 70%, and 10%, respectively, with the safety threshold (ST) set to 0.8. Candidate solutions are initialized using a uniform distribution within the predefined parameter boundaries. Following a position update, if an individual exceeds the boundary limits, it is forcibly constrained to the nearest feasible boundary. The optimization process is terminated, satisfying the convergence criteria, when the algorithm reaches the maximum number of iterations or if the change in the best fitness value remains below 1.0×10^{-6} for 10 consecutive iterations. The configuration of these hyperparameters is based on a combination of standard SSA recommendations and preliminary experimental results, aiming to balance the global exploration capability and local convergence efficiency of the algorithm.

RESULTS

Simulation Data Analysis

Internal Flow Field Analysis of the Valve

By employing Fluent computational fluid dynamics (CFD) to simulate the operational behavior of the electric control valve, a deeper understanding of its hydrodynamic performance at various valve openings can be achieved. For a comprehensive assessment, simulations were conducted at effective valve openings of 15% and 30%, specifically analyzing the pressure and velocity fields. By comparing the dynamic simulation results under these two states, and integrating the precise application requirements of boom sprayers, the control valve's opening can be flexibly modulated to achieve an optimal balance between spray performance and energy efficiency.

Fluent was utilized to model the actual working conditions of the electric control valve, extracting the internal pressure field to elucidate the static pressure distribution. The correlation between the internal pressure gradients during operation and the overall macroscopic system performance was thoroughly investigated based on these simulations. Fig. 9 and Fig. 10 illustrate the pressure contours on the symmetrical cross-sections of the valve.

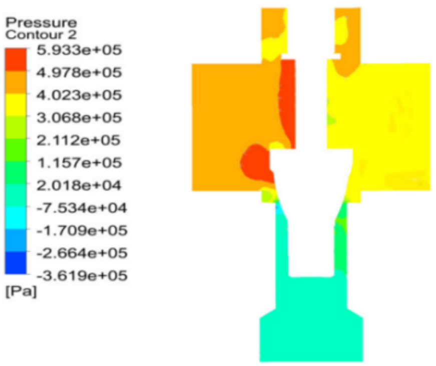

Fig. 9 - Pressure cloud map at 15% valve opening

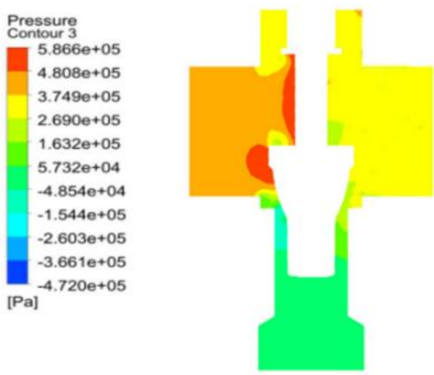

Fig. 10 - Pressure cloud map at 30% valve opening

Upon entering the valve body, the fluid pressure exhibits a highly stable state. This indicates an optimized inlet geometry design that ensures smooth fluid ingress without inducing significant pressure fluctuations, which is a critical prerequisite for the stable operation of the entire spraying system. However, as the fluid navigates through the valve core, the hydrodynamic conditions alter significantly. The physical presence of the valve core acts as a throttling obstruction, leading to a localized stagnation point and a subsequent pressure increase in the immediate vicinity of the core. This phenomenon is consistent with theoretical expectations, as the internal structure is engineered to dynamically throttle flow rate and pressure. Although this localized pressure rise is distinct, it serves as a crucial indicator of the valve's throttling efficacy. As the fluid continues its trajectory towards the outlet, it undergoes a sudden expansion, resulting in a rapid pressure drop. This continuous process functions as a "pressure dissipation" mechanism, ensuring fluid stabilization post-throttling. Once discharged from the lower outlet, the pressure profile reverts to a stable and uniform distribution.

Analysis of the Velocity Field

The velocity field characterizes the spatial distribution of fluid velocities, encompassing both the magnitude and trajectory of the flow, serving as an essential metric for describing fluid kinematics. In precision hydraulic systems, the uniformity of the velocity field directly dictates the stability of the volumetric flow rate. By thoroughly analyzing the velocity contours, the system's capability to achieve the desired flow control targets can be evaluated, thereby facilitating the optimization of the overall spraying performance. Fig. 11 and Fig. 12 present the velocity contours across the symmetrical cross-sections. It is observed that upon entering the valve body, the velocity profile exhibits a non-uniform distribution, characterized by a high-velocity core region and relatively lower velocities adjacent to the inner walls due to boundary layer friction. This initial non-uniformity induces localized turbulent vortices within the upstream chamber. However, following the flow velocity regulation at the constricted valve port, the downstream fluid velocity profile homogenizes significantly.

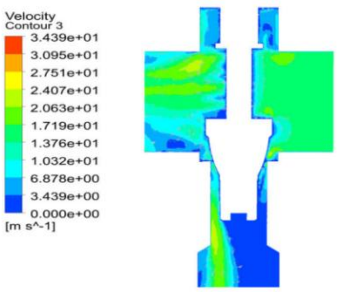

Fig. 11 - Velocity cloud map at 15% valve opening

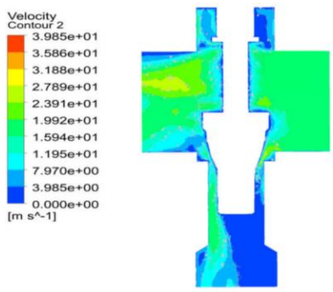

Fig. 12 - Velocity cloud map at 30% valve opening

Control System Simulation

To validate the proposed algorithms, a comprehensive simulation model of the variable-rate foliar fertilizer spraying control system was constructed using the Simulink environment in MATLAB, as shown in Fig. 13. For the transient response analysis of the automatic spraying control system, the simulation duration was set to 8.0 seconds. Based on the observed response curves and heuristic tuning, the three baseline proportional-integral-derivative parameters (K_p, K_i, K_d) were initially determined. Hardware-in-the-loop test results indicated that the intrinsic time delay— from control-signal transmission to the corresponding physical change in output flow rate—was approximately 1.0 second. Accordingly, the transport-delay block in the Simulink model was set to 1.0 seconds.

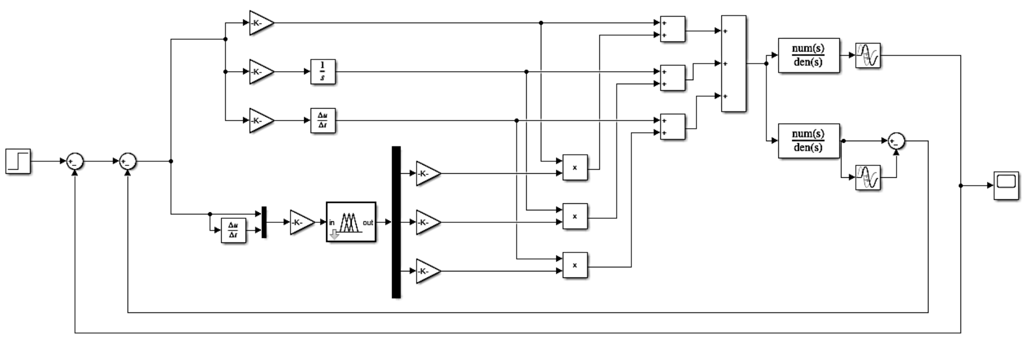

Fig. 13 - Simulink model of the variable-rate spraying control system

For the intelligent adaptive mechanism, the fuzzy controller utilizes the system error and the error change rate as input variables. The input universe of discourse was defined as [-2, 2], while the output universe of discourse for the parameter increments was constrained to [-1, 1]. Based on the fuzzy inference rules delineated in the previous section, the system quantization factors and scaling gains were strictly parameterized to satisfy the specific input-output mapping requirements of the actuator. Incorporating the empirical mathematical model derived from the Fluent CFD identification (Eq. 2), the initial baseline PID parameters were tuned to (K_p=2, K_i=10, K_d=0.5). To demonstrate the improved of the proposed algorithm, a comparative transient analysis was conducted among the conventional PID, Fuzzy PID, and the proposed ISSA-Fuzzy PID control strategies. The unit step response curves of the spraying control system under these three strategies are juxtaposed in Fig. 14.

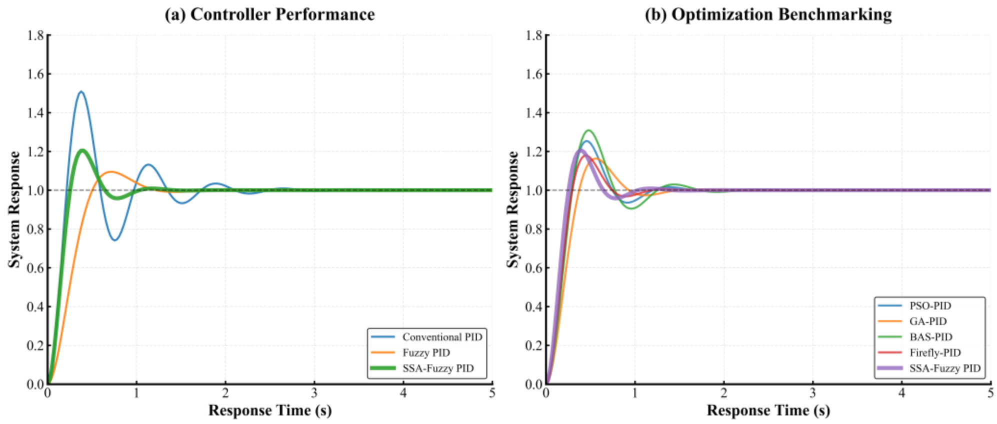

Fig. 14 - Unit step response curves of the spraying control system under different algorithms

Simulation results highlight significant performance disparities among the control strategies evaluated for the delayed second-order system (Fig. 14). As shown in the basic controller performance comparison (Fig. 14a), the conventional PID controller exhibits severe underdamped oscillations, with approximately 50% overshoot and a prolonged 2.2 s settling time, exposing its inadequacy for nonlinear hydraulic systems with pure time delays. The Fuzzy PID controller improves robustness by suppressing overshoot to 10% and reducing settling time to 1.2 s, but compromises transient speed with a slower 0.45 s rise time. Ultimately, the proposed ISSA-Fuzzy PID controller achieves the optimal dynamic balance, delivering the fastest rise time (0.35 s), an acceptable overshoot (20%), and a rapid settling time (1.0 s).

To further evaluate the performance of the Sparrow Search Algorithm, the proposed controller was benchmarked against representative swarm intelligence optimization algorithms, including PSO-PID, GA-PID, BAS-PID, and Firefly-PID (Fig. 14b). The benchmarking results demonstrate that while all intelligent algorithms mitigate the severe oscillations of the conventional PID, they exhibit varying degrees of dynamic trade-offs. BAS-PID and PSO-PID generate higher overshoots of approximately 30% and 25%, respectively. GA-PID effectively suppresses overshoot but suffers from a prolonged settling phase. Firefly-PID closely trails the proposed method; however, the ISSA-Fuzzy PID consistently demonstrates tighter overshoot control (under 20%) and the fastest convergence to the steady state.

Beyond transient response metrics, the structural advantages of the Sparrow Search Algorithm present distinct robustness benefits. While GA and PSO are prone to premature convergence in highly nonlinear hydraulic systems, and BAS struggles with multi-dimensional parameter tuning, the SSA's unique producer-scrounger-scout architecture prevents local optima trapping. This topological advantage translates into enhanced stability against sudden pressure disturbances. Furthermore, considering the limited computational resources of embedded agricultural terminals, the ISSA-Fuzzy PID algorithm provides a highly efficient alternative to advanced but computationally heavy strategies like Reinforcement Learning or Adaptive Model Predictive Control (MPC). By decoupling the global offline parameter optimization (handled by SSA) from the low-latency online adjustments (executed by the fuzzy inference engine), the real-time computational burden is reduced, supporting low-latency online execution suitable for CAN-bus-based tractor terminals. To confirm that the performance improvements observed were not due to random chance, a one-way analysis of variance (ANOVA) was performed on the settling time and overshoot data collected from the comparative tests. These results indicate that the ISSA-Fuzzy PID controller achieved the best overall balance among the tested methods, with faster convergence and tighter overshoot control than the conventional PID and the other swarm-intelligence-based controllers.

Bench Performance Tests

System Flow Rate Detection Precision Test and Data Analysis

The control accuracy of the variable-rate spraying system relies fundamentally on the measurement precision of the flow rate sensor. A bench test was conducted to calibrate the flow rate detection accuracy, ensuring that the intrinsic system error remains within permissible limits. During the experimental procedure, target flow values were transmitted via the intelligent control terminal. Simultaneously, the flow rate sensor continuously logged the dynamic flow data under operational conditions, displaying the real-time actual values on the terminal interface. To minimize random errors, the test was repeated three times. By comparing the preset target values with the actual measured values, the relative errors were calculated. The acquired data points were subsequently fitted to generate the scatter plot shown in Fig.15.

The regression analysis presented in Fig.15 reveals a coefficient of determination (R^2) of 0.995, indicating a highly significant linear correlation between the actual flow rates and the sensor-detected values. To evaluate the measurement precision and repeatability of the flow rate sensor, the experimental procedure was conducted with $n=3$ replicates for each setpoint. Statistical analysis of the absolute relative error yielded a mean of 2.14% ± 0.48%, with a 95% confidence interval (CI) of [1.62%, 2.66%]. This confined error margin and the narrow confidence interval demonstrate that the flow rate sensor provides highly reliable feedback, which exerts a minimal and statistically acceptable impact on the overall execution performance of the variable spraying control system.

System Pressure Detection Precision Test and Data Analysis

Dynamic pressure fluctuations within the hydraulic circuit can induce measurement deviations in sensor data. Consequently, the automatic spraying control system was evaluated under stable pressure environments. Pressure transmitters were installed to monitor the inlet and outlet pressures, with target values incrementally set between 200 kPa and 360 kPa. Nine distinct pressure setpoints were tested. The target setpoints and the corresponding measured values were subjected to linear regression fitting, yielding the scatter plot illustrated in Fig.16.

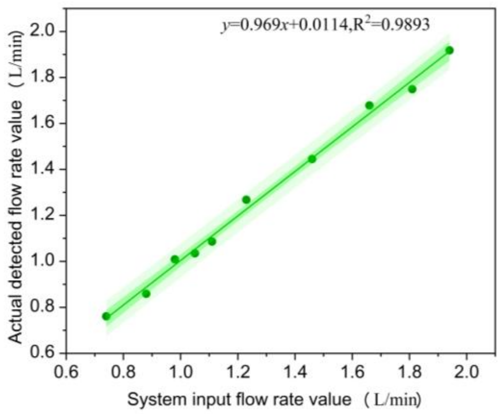

Fig. 15 - Scatter plot of flow rate detection

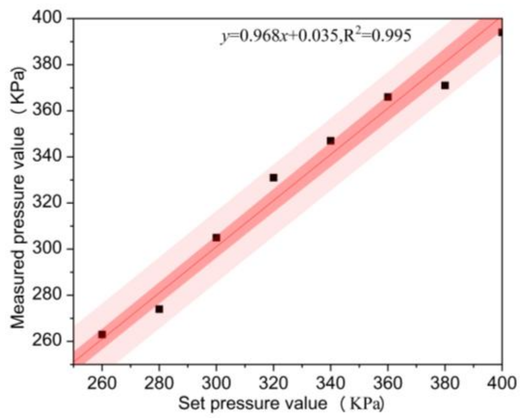

Fig. 16 - Scatter plot of pressure detection

As shown in Fig. 16, the fitted curve exhibits an (R^2) value of 0.989. To ensure repeatability, statistical analysis of the absolute relative error yielded a mean of 2.34% ± 0.52%, with a 95% confidence interval (CI) of [1.80%, 2.88%]. This acceptable and narrowly bounded pressure measurement deviation confirms that the pressure monitoring module possesses sufficient precision to support the robust operation of the spraying control system.

Electric Control Valve Core Adjustment Test and Data Analysis

During variable-rate spraying operations, the performance of the electric control valve is influenced by coupled factors, including its inherent flow regulation characteristics, sensor feedback accuracy, and the execution efficiency of the controller algorithms. These factors collectively contribute to the steady-state error between the actual applied spray volume and the target setpoint. To systematically address this, extensive adjustment tests were conducted to quantify the actuation accuracy. A metric defined as the "quantitative spraying error" was introduced, representing the arithmetic difference between the actual flow rate and the target flow rate. This error exhibits non-linear variations across different target spray flows; the specific quantitative data are detailed in Table 2.

Table 2

Quantitative spraying errors under different target spraying rates

Adjustment Direction	Set Spraying Volume (L/min)	Actual Spraying Volume (L/min)	Quantitative Spraying Error (L/min)	Relative Error (%)
Increase Spraying Flow	0.7	0.684	-0.016	-2.29
	1.0	1.021	0.021	2.10
	1.3	1.321	0.021	1.62
	1.6	1.623	0.023	1.44
	1.9	1.881	-0.019	-1.00
Decrease Spraying Flow	1.9	1.915	0.015	0.79
	1.6	1.625	0.025	1.56
	1.3	1.276	-0.024	-1.85
	1.0	1.019	0.019	1.90
	0.7	0.685	-0.015	-2.14

Furthermore, the transient relationship between the dynamic valve adjustment process and the system output flow was established. Time-domain response curves for stepwise increasing and decreasing flow rates were plotted, as shown in Fig. 17 and Fig. 18.

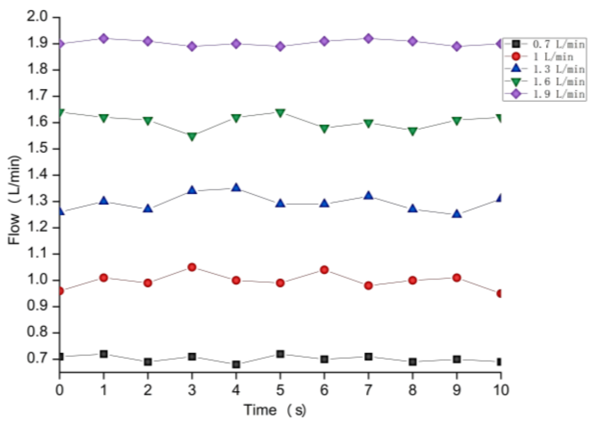

Fig. 17 - Time-domain response curve for increasing flow rate

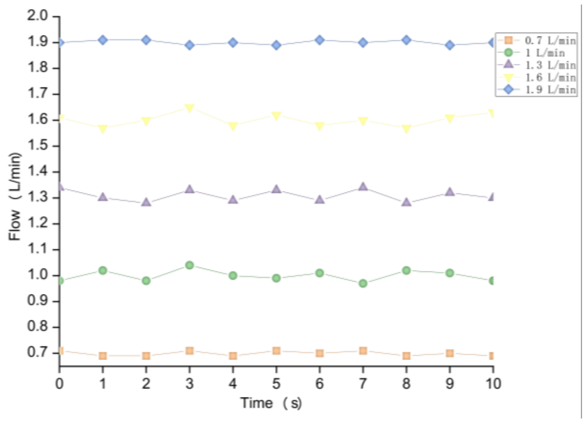

Fig. 18 - Time-domain response curve for decreasing flow rate

The transient profiles in Fig. 17 and Fig. 18 suggest that the pulsatile pressure application from the diaphragm pump inherently influences the output flow rate and pipeline pressure. Time-series data analysis confirms that the flow rate output fluctuates synchronously with periodic pressure pulsations. When the electric valve opening is small, the elevated hydraulic resistance dampens these pulsations, minimizing output flow fluctuations. Conversely, when the valve is fully open, the flow resistance is minimized, allowing the fluid to stabilize quickly, thereby achieving a stable high-flow output state.

ISSA-Fuzzy PID Control Algorithm Test and Data Analysis

The automatic spraying control system exhibits inherent time-delay and overshoot characteristics, which strictly compromise the precision of variable-rate field operations. To overcome this engineering bottleneck, the ISSA-Fuzzy PID control algorithm is deployed to counteract the pure lag effect, integrating a fuzzy inference module to diminish the system's sensitivity to external parameter variations, thereby achieving real-time, robust, and stable flow control.

To empirically evaluate the response stability of the hardware system driven by the ISSA-Fuzzy PID algorithm, pressure disturbance tests were executed. The reference system pressures were explicitly set to 250 kPa, 300 kPa, and 350 kPa. During the tests, the dynamic feedback data were continuously logged and exported via a CAN bus monitoring software. Data analysis corroborates that the system rapidly attains steady-state convergence under all three pressure conditions. The comparative dynamic characteristic curves are illustrated in Fig. 19.

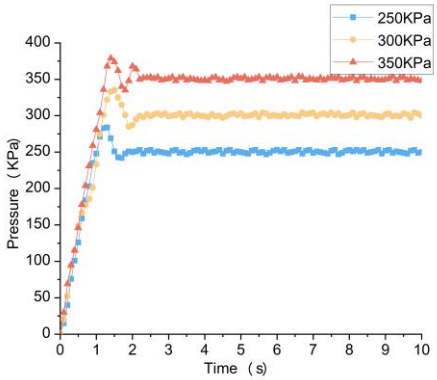

Fig. 19 - Dynamic response curves under different reference pressures

In summary, the ISSA-Fuzzy PID control algorithm demonstrates adaptive performance capabilities across varying operational pressures. At a target pressure of 250 kPa, the system exhibited a restrained overshoot of 7.12% coupled with a swift rise time of 1.1 seconds. Upon increasing the set pressure to 300 kPa, the overshoot optimally decreased to 6.67%, while the rise time slightly extended to 1.3 seconds. At the maximum tested pressure of 350 kPa, the overshoot further narrowed to 6.29%, maintaining a consistent rise time of 1.3 seconds. These empirical findings indicate that the ISSA-Fuzzy PID control architecture effectively suppresses overshoot while ensuring improved transient response rapidity across a broad spectrum of pressure settings, significantly enhancing both the steady-state stability and dynamic efficiency of the automated spraying system.

To further quantify the robustness of the ISSA-Fuzzy PID controller, performance metrics (overshoot and rise time) were evaluated across 10 independent simulation trials under stochastic pressure disturbances. The ISSA-Fuzzy PID controller achieved a mean overshoot of 6.69% with a 95% confidence interval (CI) of [6.40, 6.98] %. Compared to conventional PID, the ISSA-Fuzzy PID showed a significantly shorter mean settling time ($p < 0.05$ via one-way ANOVA), confirming that the proposed algorithm significantly improves control consistency and reliability for agricultural actuating systems.

While these bench experiments validate the hardware integration and algorithmic precision, several limitations inherent to laboratory environments must be acknowledged. The current evaluations were conducted under stable ambient temperatures utilizing homogeneous fluid properties. In practical field operations, soybean foliar fertilizers exhibit varying viscosities, and fluctuating ambient temperatures can alter hydraulic fluid dynamics. Additionally, real-world field conditions introduce mechanical vibrations from the tractor, irregular power take-off (PTO) speeds, and sensor noise induced by canopy shading or sloped terrain. Therefore, although the 1.9 s dynamic pressure regulation achieved in this study demonstrates strong technical feasibility at the bench scale, the comprehensive agronomic benefits—specifically regarding canopy fertilizer deposition, nutrient uptake efficiency, and ultimate yield improvements—require extensive multi-year field trials under complex, unstructured agricultural environments.

CONCLUSIONS

To address control-precision limitations in soybean foliar-fertilizer variable-rate spraying, this study designed an automatic real-time variable-rate control system. Based on CFD simulation, controller modeling, and bench-scale validation, the following conclusions are drawn:

(1) A second-order transfer function of the electric control valve was derived through system identification via CFD dynamic mesh simulations. Hydrodynamic analyses at 15% and 30% openings characterized the internal throttling behavior. An ISSA-Fuzzy PID control strategy was proposed to mitigate system time-delay; MATLAB/Simulink simulations verified that, under modeled bench conditions, this algorithm improved transient response, overshoot suppression, and stability compared with conventional PID and standard Fuzzy PID controllers.

(2) Bench tests validated hardware integration accuracy, with average relative errors of 2.14% and 2.34% for flow-rate and pressure detection, respectively. Hardware validation confirmed that the ISSA-Fuzzy PID algorithm achieved dynamic target-pressure regulation within 1.9 s. While these results demonstrate the technical feasibility of the proposed system at a bench scale, the performance of the system in terms of field-scale spraying stability, actual fertilizer-use efficiency, and agronomic yield impacts remains to be validated in future on-farm trials.

ACKNOWLEDGEMENT

This work was supported by the 2023 Key Research and Development Program of Heilongjiang Province under Grant No. 2023ZXJ07B02.

REFERENCES

[1] Dhanya, V.G., Subeesh, A., Kushwaha, N.L., Vishwakarma, D.K., Nagesh Kumar, T., Ritika, G., Singh, A.N. (2022). Deep learning based computer vision approaches for smart agricultural applications. *Artificial intelligence in agriculture* 6, 211-229.

[2] Dong, X., Li, R., Wang, M., Zhang, X., Yu, S., Xue, J. (2025). Design and research of variable fertilization system for rice based on bilinear interpolation. *INMATEH-Agricultural Engineering*. Vol.77(3), 1519-1531.

[3] Farooque, A.A., Hussain, N., Schumann, A.W., Abbas, F., Afzaal, H., McKenzie-Gopsill, A., Esau, T., Zaman, Q., Wang, X. (2023). Field evaluation of a deep learning-based smart variable-rate sprayer for targeted application of agrochemicals. *Smart agricultural technology,* 3, 100073.

[4] Jiao, Y., Zhang, S., Jin, Y., Cui, L., Chang, C., Ding, S., Sun, Z., Xue, X. (2025). Research progress on intelligent variable-rate spray technology for precision agriculture. *Agronomy-Basel,* 15(6), 1431.

[5] Karimi, A., Garcia, D., Longchamp, R., (2004). Pid controller tuning using Bode's integrals. *IEEE Trans. Control Syst. Technol*. 11(6), 812-821.

[6] Kumar, S., Tewari, V.K., Bharti, C.K., Ranjan, A. (2021). Modeling, simulation and experimental validation of flow rate of electro-hydraulic hitch control valve of agricultural tractor. *Flow Meas. Instrum*. 82, 102070.

[7] Patle, R., Kavitha, R., Surendrakumar, A., Sahni, R.K., Suthakar, B., Kannan, B., Maragatham, S. (2025). Development of a sensor-based embedded system for on-the-go variable-rate fertilizer applicator in maize crop. *Results Eng*. 28, 107852.

[8] Pawase, P.P., Nalawade, S.M., Bhanage, G.B., Walunj, A.A., Kadam, P.B., Durgude, A.G., Patil, M.R. (2023). Variable rate fertilizer application technology for nutrient management: a review. *Int. J. Agric. Biol. Eng.* 16(4), 11-19.

[9] Su, D., Yao, W., Yu, F., Liu, Y., Zheng, Z., Wang, Y., Xu, T., Chen, C. (2022). Single-neuron PID UAV variable fertilizer application control system based on a weighted coefficient learning correction. *Agriculture*-Basel 12(7), 1019.

[10] Wu, X., Zhang, L., Zhao, J., Hu, X. (2026). Control system based on tuna swarm optimization, fuzzy PID, and MQTT protocol for remote fertilization. *Agriculture* 16(11), 1206.

[11] Xie, L., Mao, W., Zhang, X., Du, Y., Fang, X., Zhou, C. (2026). Study on the variable side - deep fertilization control system for rice based on soil electrical conductivity. *Front. Plant Sci*. 17, 1748101.

[12] Xu, C., Xie, F., Tian, Z., Zhao, Z., Chen, Z., Li, Y. (2025). Fuzzy PID control strategy optimised by sparrow search algorithm for digital proportional valve with differential control of dual high-speed on/off valves. *Int. J. Hydromechatron*. 8(4), 444-467.

[13] Xu, Y., Jin, Y., Sun, Z., Xue, X. (2025). Pso-based system identification and fuzzy-PID control for EC real-time regulation in fertilizer mixing system. *Agronomy*-Basel 15(5), 1259.

[14] Xue, J., Shen, B. (2020). A novel swarm intelligence optimization approach: sparrow search algorithm. *Syst. Sci. Control Eng*. 8(1), 22-34.

[15] Yuxuan, J., Zhu, S., Yongkui, J., Longfei, C., Zhang, X., Wang, S., Songchao, Z., Chang, C., Suming, D., Xinyu, X., (2025). Current status and future prospects of key technologies in variable-rate spray. *Agriculture* 15(20), 2111.

[16] Zhang, W., Tong, J., Zhang, F., Zhang, W., Zhang, J., Zhang, J., Zhang, J., Sun, H., Northwood, D.O., Waters, K.E., Ma, H., (2025). Integrated irrigation of water and fertilizer with superior self-correcting fuzzy PID control system. *Plos One,* 20(5), e324448.

[17] Zhu, F., Zhang, L., Hu, X., Zhao, J., Meng, Z., Zheng, Y., (2023). Research and design of hybrid optimized backpropagation (BP) neural network PID algorithm for integrated water and fertilizer precision fertilization control system for field crops. *Agronomy*, 13(5), 1423.